

Multiple-beam fibre reflection interferometer based on an all-dielectric diffraction structure

V.S. Terentyev, V.A. Simonov

Abstract. We report experiments aimed at making a fibre reflection interferometer based on all-dielectric diffraction structures for the range 1500–1600 nm. The diffractive scattering structure of the input mirror of the interferometer is produced on the fibre end face by damaging it using abrasive diamond film with a grain size of a few microns. As a result, sharp reflection peaks are obtained for two interferometers, with the following parameters: finesse, 100 and 11; contrast, 2 and 60, respectively. Such an interferometer can, in principle, combine high contrast and high finesse.

Keywords: multiple-beam reflection interferometer, diffraction, fibre optics, single-mode fibre.

1. Introduction

A multiple-beam two-mirror reflection interferometer [1, 2] is of interest for ensuring single-frequency operation of short-cavity fibre lasers or laser diodes [3]. Traditionally, longitudinal mode selection in fibre lasers is brought about by fibre Bragg gratings, Fabry–Perot (FP) filters, ring cavities and their cascades (Vernier effect), reflective diffraction gratings etc. [4]. The use of a reflection interferometer offers some advantages, the most useful of which is probably the possibility of operation in reflected light. This can be ensured by adding losses to the structure of the cavity input mirror (on the light source side), which leads to asymmetry in its reflectance. Moreover, a reflection interferometer can offer a high degree of radiation selection, comparing well to a Fabry–Perot interferometer (FPI), and have a relatively simple design. When a reflection interferometer is used as a mirror, the base of the linear laser cavity [3] can be made much shorter (under 100 μm), which allows one to select one longitudinal mode of the cavity, cancelling out the effect of mode competition in a wide spectral range. On the other hand, the spacing between cavity eigenmodes becomes very large, and changing the base length of even one interferometer leads to a transition to a neighbouring longitudinal mode, which means that continuous laser wavelength tuning becomes impossible. At the same time, in contrast to traditional selection schemes, such a scheme can, in principle, ensure fine (continuous) laser wavelength tuning in a very wide (~ 100 nm) spectral range and

with a high rate (~ 1 kHz) if concurrent adjustment of the interferometer and cavity bases is ensured.

This paper examines an all-dielectric reflection interferometer in single-mode fibre, which contains no absorbing elements in its structure, in contrast to previously proposed configurations based on a thin metallic film [5–7]. The interferometer has a dielectric scatterer on the fibre end face, which ensures the highest possible optical damage resistance of its structure and makes it suitable for use at high optical powers. The limiting input power W_{max} at which a multiple-beam interferometer is capable of operating can be estimated as the ratio of the power W starting at which nonlinear effects in optical fibre cannot be neglected to the interference fringe finesse: $W_{\text{max}} = W/F$. This is due to the increase in the amplitude of the optical field in the fibre base between the interferometer mirrors at resonance. The characteristic threshold power W for nonlinear effects in standard single-mode fibres is several tens of watts. For example, the Micron Optics FFP-TF2 tunable FP fibre filter, with a fringe finesse $F = 200$, has $W_{\text{max}} = 100$ mW. In specialised single-mode fibres, W can be increased by reducing intensity via an increase in mode field diameter.

A 3D configuration of a diffractive reflection interferometer (DRI) has been known for a relatively long time [8]. It has a noninverted spectral response function in reflection, similar to that of an FPI in transmission, which has the form of narrow spectral reflection peaks on a lower background. Previous work demonstrated the conceptual feasibility of obtaining an DRI on the end face of optical fibre [5], but imperfection of the modifications obtained and the lack of a light-guiding interferometer base made it impossible to obtain at least partially suitable characteristics. Later on, we demonstrated noninverted spectral interference picture of a fibre FPI with a damaged input mirror [9], but it had low fringe finesse (about 4) and low contrast (about 2). In addition, there was no technology of obtaining such a noninverted picture, because the observed effect was basically a consequence of an accidental error in the fabrication of the FP filter. At the presence stage, DRI fabrication technology requires that the scatterer geometry and characteristics be determined and that methods of the fabrication of such modifications in single-mode fibre be searched for.

The purpose of this work is to demonstrate a new experimental method for the fabrication of an DRI in single-mode fibre, which may become the basis for further development of the technology of fibre reflection interferometers. The essence of the method is to modify the end face of single-mode optical fibre that is coupled with a Gires–Tournois (GT) interferometer. The response function then contains a noninverted

V.S. Terentyev, V.A. Simonov Institute of Automation and Electrometry, Siberian Branch, Russian Academy of Sciences, prosp. Akad. Koptyuga 1, 630090 Novosibirsk, Russia; e-mail: terentyev@iae.nsk.su

Received 23 June 2017; revision received 1 August 2017
Kvantovaya Elektronika 47 (10) 971–976 (2017)
Translated by O.M. Tsarev

spectral dependence of reflectance. Among possible modifications of the fibre end face, we are interested in those which ensure higher fringe contrast and finesse.

2. Theoretical description

Due to the distinctive features of the experimental problem, a three-mirror cavity is considered in the general case to describe the spectral properties of an interferometer. As shown in Fig. 1a, the cavity consists of three mirrors: M0, M1 and M2. M0 is a scattering mirror, which introduces diffraction losses for the fundamental mode of the fibre. In addition, in the air gap l_0 between mirrors M0 and M1 there are losses due to the diffraction divergence of the light wave, which reduce the amplitude of the fundamental mode. To take into account the effect of these losses, we introduce a coefficient that represents the decrease in amplitude per pass through the air gap, $\sqrt{T_0}$ ($0 \leq T_0 \leq 1$), which depends on l_0 and can be evaluated analytically using formulas from Marcuse [10]. The fibre cavity between mirrors M1 and M2 is taken to have no propagation loss (the region between the mirrors possesses guidance properties and the loss can be neglected at such small lengths). The M1–M2 cavity is a GT interferometer in which one of the mirrors (M2) has high reflectance (near 100%) and the other (M1) has lower reflectance.

Each mirror is characterised by the amplitude reflection coefficients on both sides, which may differ in the general case, when there are losses in the mirrors. In the plane wave approximation, the amplitude reflection (\tilde{r}_3) and transmission (\tilde{t}_3) coefficients of a three-mirror multiple-beam interferometer at normal incidence can be represented using formulas for a two-mirror interferometer [1]:

$$\tilde{r}_3 = r_{01} + \frac{T_0 t_{01} t_{02} \tilde{r}_2 \exp(-i2\psi_0)}{1 - T_0 r_{02} \tilde{r}_2 \exp(-i2\psi_0)}, \quad (1)$$

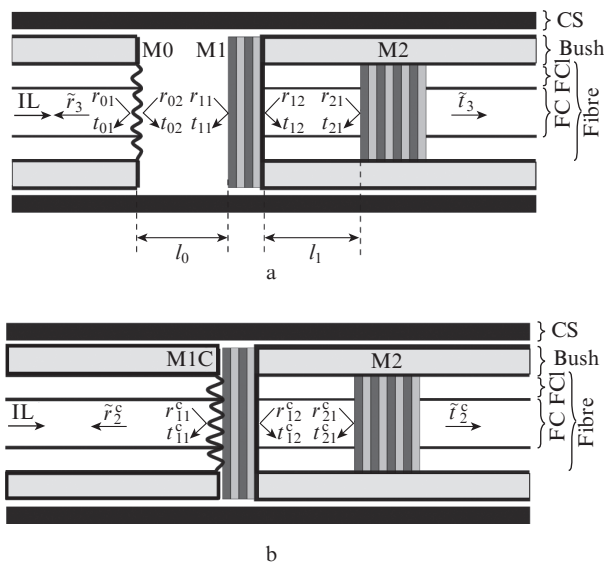


Figure 1. Fibre DRI configurations at (a) $l_0 > 0$ and (b) $l_0 = 0$: M0, M1 and M2 are cavity mirrors; M1C is a composite mirror; r_{jk} and t_{jk} are the amplitude reflection and transmission coefficients of the cavity mirrors; r_{jk}^c and t_{jk}^c are the coefficients of mirror M1C ($j = 0, 1, 2$; $k = 1, 2$); \tilde{r}_3 , \tilde{t}_3 , \tilde{r}_2^c and \tilde{t}_2^c are those of the DRI; IL is incident light; FC is the fibre core; FCl is the fibre cladding; and CS is a cylindrical spring.

$$\tilde{t}_3 = \frac{\sqrt{T_0} t_{01} \tilde{t}_2 \exp(-i\psi_0)}{1 - T_0 r_{02} \tilde{r}_2 \exp(-i2\psi_0)}, \quad (2)$$

$$\tilde{r}_2 = r_{11} + \frac{t_{11} t_{12} r_{21} \exp(-i2\psi_1)}{1 - r_{12} r_{21} \exp(-i2\psi_1)}, \quad (3)$$

$$\tilde{t}_2 = \frac{t_{11} t_{21} \exp(-i\psi_1)}{1 - r_{12} r_{21} \exp(-i2\psi_1)}, \quad (4)$$

where the amplitude coefficients of the mirrors, $r_{jk} = \sqrt{R_{jk}} \times \exp(i\Psi_{jk})$ and $t_{jk} = \sqrt{T_{jk}} \exp(i\Phi_{jk})$ ($j = 0, 1, 2$; $k = 1, 2$), are expressed through the power reflection (R_{jk}) and transmission (T_{jk}) coefficients and their phases Ψ_{jk} and Φ_{jk} ; $\psi_0 = 2\pi l_0/\lambda$; $\psi_1 = 2\pi l_1 n/\lambda$; n is the refractive index of the base of the Gires–Tournois interferometer resonator (GTR) (if there is a fibre base, the refractive index should be equal to the effective refractive index of the fibre mode); l_1 is the base length; and λ is the incident light wavelength. The first subscript (j) refers to the number of the mirror, and the second (k), to its side (1, the side of incidence; 2, the opposite side). The power reflection and transmission coefficients of the interferometer are $\tilde{R}_3 = |\tilde{r}_3|^2$ and $\tilde{T}_3 = |\tilde{t}_3|^2$, respectively.

Formulas (1)–(4) are applicable to an interferometer with losses in its mirrors, so they will be generally valid for describing the properties of an interferometer at $R_{jk} + T_{jk} < 1$. In such a case, the physical nature of the losses in its mirrors (absorption or scattering) is unimportant.

As follows from the theory of a two-mirror reflection interferometer [1], to obtain a high-contrast noninverted spectral dependence of reflectance in reflection from a GTR (Fig. 1a) it is necessary that the input mirror M1 have a high asymmetry in its reflectances. In other words, mirror M1 should have high losses on side 1. Such losses can be ensured e.g. using a scattering mirror M0 in the three-mirror configuration under consideration if it is brought closer to M1. At $l_0 = 0$, it is convenient to consider a composite mirror, M1C, and the three-mirror configuration transforms into a two-mirror one (Fig. 1b). Since the optical coefficients of mirror M1C can differ significantly from those of M1, it is reasonable to introduce its own coefficients: $r_{jk}^c = \sqrt{R_{jk}^c} \exp(i\Psi_{jk}^c)$ and $t_{jk}^c = \sqrt{T_{jk}^c} \exp(i\Phi_{jk}^c)$. The reflectances of mirror M1C should meet the conditions

$$0 \approx R_{11}^c \ll R_{12}^c < R_{21}^c \rightarrow 1. \quad (5)$$

The response functions of the two-mirror interferometer based on mirrors M1C–M2 in reflection \tilde{r}_2^c and transmission \tilde{t}_2^c will have the form (3) and (4) after the changes $r_{1k} \rightarrow r_{1k}^c$ and $t_{1k} \rightarrow t_{1k}^c$.

In the general case, the shape of the spectral dependence of the response function of a reflection interferometer for $R_{11}^c > 0$ can have significant asymmetry [1]. Unlike in the case of an FPI, in a reflection interferometer the shape of bands in reflection can be controlled using the following relation between the phases of mirror M1C: $\theta^c = \Psi_{11}^c + \Psi_{12}^c - 2\Phi_{11}^c$. The bands are totally symmetric at $\theta^c = m\pi$ (where m is an integer). Thus, to obtain a given spectral dependence in fabricating a scatterer, both the power coefficients of mirror M1C and their phases should have certain values.

3. Fabrication of DRIs

The problem of introducing controlled losses for producing a scatterer with tailored properties is difficult technologically and was not posed at this stage. We used a simple way to introduce losses by damaging the fibre end face (M0) with an abrasive film having a grain size on the order of a few microns. This procedure reduced the reflectance of the end face. Next, the damaged fibre was brought to mirror M1 of the GTR and the reflection spectrum was observed in a range exceeding the free spectral range of the GTR ($\Delta\lambda > 11$ nm). The value of $\Delta\lambda$ (the spacing between neighboring interference minima) was determined from the spectral dependence of the GTR in reflection using the intact mirror M0. The end face was damaged further until a noninverted spectral dependence of reflectance was obtained.

Experimental DRIs each consist of two ceramic bushes centred by a cylindrical spring (CS) (Fig. 1). The fibre with the damaged end face is located in the left bush, and the GTR, in the right bush. We fabricated two GTRs. One had a high-finesse resonator and the other had a lower finesse resonator. The finesse was determined by the reflectances of the GTRs' mirrors. Their parameters are as follows:

GTR (M1–M2)	No. 1	No. 2
Base $l_1/\mu\text{m}$	70.7	84.6
Mirror M1, M_1 ($R_{11} = R_{12}$)	7 (0.944)	3 (0.667)
Mirror M2, M_2 (R_{21})	15 (0.998)	13 (0.997)

Here $M_{1,2}$ is the number of quarter-wave layers in the multilayer structure $\{\text{TiO}_2, (\text{SiO}_2, \text{TiO}_2)^{(M_i-1)/2}\}$, $i = 1, 2$. The numbers in round brackets indicate calculated reflectances. The length of the GTR base was determined as $l_1 = \lambda^2/(2\Delta\lambda n)$, where $n = 1.4682$ (the effective refractive index of the fundamental mode of SMF-28e fibre).

The GTRs were fabricated using SMF-28e single-mode fibre. After the fibre end face was sequentially polished with abrasive diamond films having a grain size of 3, 1 and 0.02 μm , a multilayer dielectric coating consisting of M_2 layers (mirror M2) was grown on the end face via the magnetron sputtering of Ti and Si in an argon–oxygen atmosphere. Given the errors made in producing the quarter-wave layers, the actual reflectance might be slightly lower than those indicated above. In producing mirror M2 of GTR 1, we used an 80- μm -diameter hole mask located at the centre of the fibre axis. At the same time, because of the possible displacement of the mask and its considerable thickness, mirror M2 was nonuniform in core area. This led to a significant polarisation dependence of mirror parameters, which was, however, not critical for the purposes of this study. Despite the small fibre core diameter (8.2 μm), its area is readily distinguishable in transmitted white light under a 400 \times fibre microscope when the fibre end face is illuminated from the reverse side. In the same way, it was easy to assess the uniformity of the interference coating of mirror M2, which yielded various blue-green tinges over the core area when observed in reflected light from the illumination of the fibre microscope on the air side (third harmonic of $\lambda = 1550$ nm light). Mirror M2 of GTR 2 had no visually detectable nonuniformity, because it was fabricated by a different technique (with no mask).

A fibre segment with mirror M2 was placed in the right bush (inner diameter, 125.5 μm) and sealed by epoxy, and the fibre emerging on the M1 side was broken off. To fabricate mirror M1, the right bush was also polished and M_1 dielectric layers were produced on its end face.

Mirror M0 first had the form of the end face of single-mode fibre sealed by epoxy in the left bush and polished. Diffraction losses that would ensure asymmetry of reflection from mirror M1C were introduced by intentionally damaging the end face (M0) with abrasive film having a grain size of 1, 3, 5 or 9 μm . A successful damage criterion was a decrease in reflectance back to the fibre, which was expected to help reduce reflectance R_{11}^c . The variation of reflection from the end face was monitored in real time on a Yokogawa AQ 6370 optical spectrum analyser in a spectral range as narrow as ~ 1 nm, which allowed us to obtain several measurements per second. After having been damaged, the end face was cleaned with a propanol-wetted viscose napkin. The best result was obtained in the case of the film with a grain size of 5 μm . The reflectance was about 0.3% (the reflectance of the intact end face was 3.5%), and narrow bands of high reflection orders were observed in the interferometer (noninverted interference pattern).

4. Experimental setup

The characteristics of the DRI were measured using the setup schematised in Fig. 2. As a light source, we used a superluminescent diode with a centre wavelength of 1550 nm. The full width at half maximum of its spectrum was 40 nm. The output of the source had a low degree of polarisation (8%), which was measured by a Thorlabs TXP 5004 polarimeter with the use of a PAN5710IR3 sensor head. The DRI was located at output 2 of the fibre circulator and was connected through an FC/PC fibre butt joint (BJ). The \tilde{R}_3 and \tilde{R}_2^c reflectance spectra were measured through output 3. Transmittances \tilde{T}_3 and \tilde{T}_2^c could be measured through the GTR output. Reflection spectra were normalised to the reflectance of the free end of the BJ (3.5%), matched to output 2 of the circulator (the BJ was then disconnected). The spectra were recorded using a Yokogawa AQ 6370 spectrum analyser with an optical resolution of 0.02 nm. In our experiments, we varied the spacing

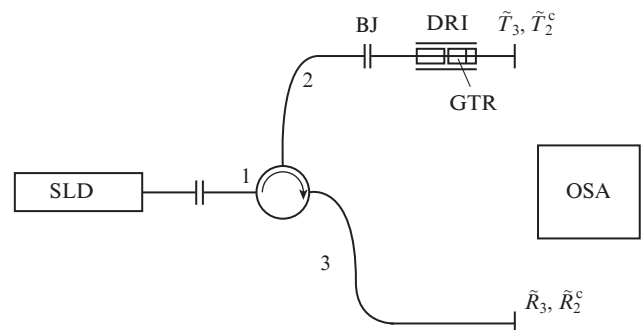


Figure 2. Schematic of the measurement of the spectral characteristics of the DRI:

(SLD) superluminescent diode; (BJ) fibre butt joint; (DRI) diffractive reflection interferometer; (GTR) Gires–Tournois resonator; the reflectances and transmittances of the DRI are \tilde{R}_3 , \tilde{T}_3 ($l_0 > 0$) and \tilde{R}_2^c , \tilde{T}_2^c ($l_0 = 0$); (OSA) optical spectrum analyser.

l_0 between mirrors M0 and M1 and examined the transformation of the reflection spectra.

5. Discussion of results

Figure 3 presents measured reflection spectra of DRI 1 (based on GTR 1) for three cases of damage to the end face of mirror M0. In each set of spectral dependences, we can distinguish two interference components differing in nature. One component is due to the M0–M1 resonator, with a base $l_0 > 0$, and has a characteristic, low-finesse sinusoidal shape [curves (1), (2)]. The other has only sharp peaks (dips), with a mode spacing and finesse characteristic of GTRs [curves (3), (4)]. In all spectra, the spectral position of the narrow peaks (dips) is independent of l_0 . In all cases, within one free spectral range the main, high peak has a nearby additional weak peak due to the polarisation dependence of the GTR, which seems to be related to the polarisation nonuniformity of mirror M2 or the birefringence of the fibre base. There are a few significant sources of the polarisation dependence in a fibre resonator: birefringence of the fibre material, birefringence induced by the stress that resulted from cementing (torsion and radial stress), and nonuniformity of the reflection phase of the mirrors. In our opinion, the last factor is the most likely in the

case under consideration. Such nonuniformity may result from three independent effects: nonuniform growth of the dielectric layers of mirrors M1C and M2, inadequate polishing of the surface of the end faces (with parallel scratches left on them) or polarisation dependence of the scatterer. In the presence of any nonuniformity, the overlap integral of the fundamental mode of the fibre will depend on whether the polarisation vector is oriented along or across the nonuniformity direction, which will lead to a difference between the reflection phases of the mirrors for each polarisation [the reflection phase of the mirrors appears in the total phase shift between mirrors M1 and M2: $\varphi_1 = \psi_1 - (\Psi_{12}^c + \Psi_{21})/2$]. In addition, the combined phase θ^c , determining the shape of the spectral dependence of reflection, may be polarisation-dependent [1].

Figure 3a illustrates the transformation of the reflection spectra at various l_0 values in the case of the intact cavity mirror M0. At $l_0 \neq 0$, the loss parameter T_0 in (1) and (2) is small and is dominated by the loss due to the diffraction divergence in the air gap, so the maximum value of \tilde{R}_3 decreases with increasing l_0 , as expected. At $l_0 = 0$ ($\tilde{R}_3 \equiv \tilde{R}_2^c$), we observe an inverted picture, with narrow dips, characteristic of FPIs in reflected light. In this case, it can be thought that the input composite mirror M1C has no losses and no significant asymmetry in its reflectances, i.e. $R_{11}^c = R_{12}^c$, $\Psi_{11}^c = \Psi_{12}^c = \pi$, $T_{11}^c = T_{12}^c$ and $\Phi_{11}^c = \Phi_{12}^c = \pi/2$.

Figure 3b shows reflection spectra of DRI 1 after mirror M0 was damaged by abrasive film with a grain size of 3 μm . The shape of the spectra changed only slightly. Because of the additional scattering loss at $l_0 = 0$, the maximum reflectance decreased, and the phase changes in the reflectance and transmittance of mirror M0 led to a decrease in the interference dips.

Damaging the mirror with abrasive film having a grain size of 5 μm (Fig. 3c) is seen to cause significant changes in the shape of the spectra at $l_0 = 0$, producing strong, sharp peaks on a lower background [spectrum (4)]. Note that the shape of spectra (1) and (2) is qualitatively similar to that of spectra (1) and (2) at $l_0 > 0$ in the above two cases (Figs 3a, 3b). Spectrum (3), obtained at a rather small l_0 ($\sim 5 \mu\text{m}$) (as estimated from the spectral nonuniformity of the background) has an average background level above that of spectrum (4). Judging from the noninverted shape of spectrum (4), the composite mirror M1C is asymmetric with respect to reflection, unlike M1.

Remarkably, a noninverted interference pattern is present in all spectra (2) in Fig. 3, albeit with different maximum reflectances. All these spectra have a sharp, narrow peak near the reflection minimum, even in the case of the intact end face (near 1520 and 1565 nm in Fig. 3a and near 1530 and 1555 nm in Fig. 3b). This is probably difficult to obtain in the case of bulk components, but is easy to realise in the case of single-mode fibre, even without introducing losses directly into mirror M0 (reflection asymmetry in the M0–M1 system is ensured by losses in the case of double propagation of light through the air gap between M0 and M1). This effect can be used to resolve problems in which the total reflection loss level is unimportant, but it is necessary to have optical filtering in a narrow spectral range.

Figure 4 shows spectral dependences of reflectance in the range 1515–1535 nm for DRI 1 and DRI 2 at $l_0 = 0$. The shape of the spectral dependence of reflectance for DRI 2 remains unchanged throughout the range 1500–1600 nm. Also shown in Fig. 4 is a calculated $\tilde{R}_2^c(\lambda)$ curve, set by for-

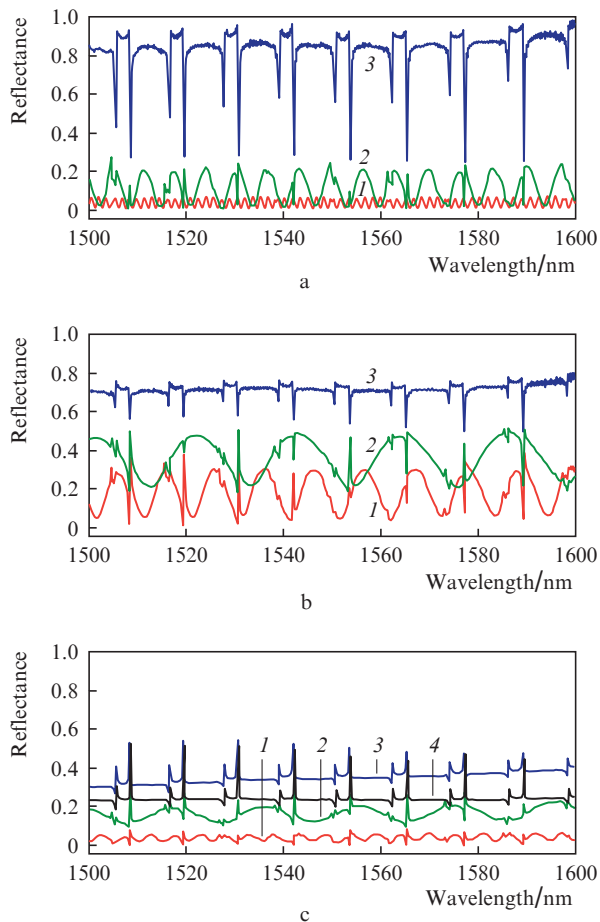


Figure 3. Spectral dependences of the reflectances \tilde{R}_3 of the DRI: (a) intact end face at $l_0 = (1)$ 761, (2) 184 and (3) 0 μm ; (b) damaged end face (3- μm abrasive film) at $l_0 = (1)$ 116, (2) 56 and (3) 0 μm ; (c) damaged end face (5- μm abrasive film) at $l_0 = (1)$ 235, (2) 62, (3) 5 and (4) 0 μm .

mula (3), for a two-mirror interferometer with mirrors M1C and M2. The parameters of the mirrors in the DRIs were determined by numerical calculation using the function `curve_fit` in the SciPy library for Python (Table 1).

Table 1.

RDI	$l_1/\mu\text{m}$	R_{11}^c	Ψ_{11}^c/rad	R_{12}^c	Ψ_{12}^c/rad	T_{11}^c	Φ_{11}^c/rad	R_{21}
1	70.7	0.238	1.12π	0.945	0.14π	0.007	1.64π	0.994
2	84.5	0.062	0.33π	0.656	0.87π	0.088	0.34π	0.971

The above power reflection and transmission coefficients approach those expected for experimentally fabricated samples. The calculated curves in Figs 4a and 4b describe well the narrow, strong peaks in the experimentally determined dependences of reflection. The finesse of the interference fringes F_1 for DRI 1, which in the case of a reflection interferometer is calculated as the ratio of the free spectral range of the interferometer, $\Delta\lambda$, to the spectral width of the reflection peak, $\delta\lambda$, at half maximum, $(\tilde{R}_{\max}^c + \tilde{R}_{\min}^c)/2$ relative to \tilde{R}_{\min}^c , is about 100 and is determined by the GTR finesse. The fringe contrast of DRI 1 is rather low: $\tilde{R}_{\max}^c/\tilde{R}_{\min}^c \approx 2$. The fringe finesse F_2 of DRI 2 is not so high ($F_2 \approx 11$), but the contrast is substantially higher (~ 60). Both samples have considerable reflection losses (near 50% and above 65%, respectively). The deviation of the experimental dependences from the calculation results in the case of DRI 1 is due to the polarisation dependence,

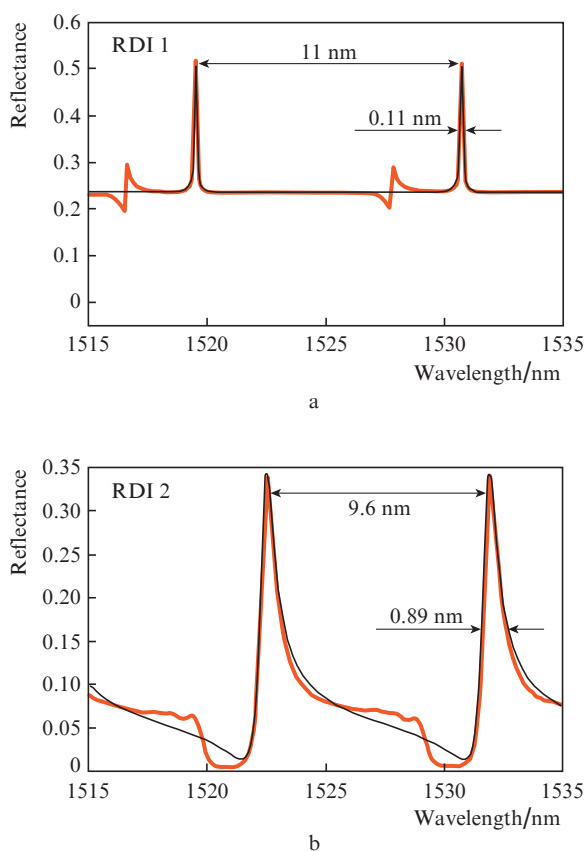


Figure 4. Spectral dependences of reflectance \tilde{R}_2^c for (a) high-finesse DRI 1 and (b) low-finesse DRI 2. The thick lines represent the experimental data and the thin lines represent the calculation results.

which shows up as small Z-shaped peaks shifted in wavelength relative to the strong peaks and having a different shape, which is associated with the polarisation dependence of the combined phase θ^c of the input mirror M1C because of the presence of the axially asymmetric scatterer. In the case of DRI 2, the deviation is much smaller and shows up only in low-reflectance regions. The results presented in Fig. 4 indicate that, in principle, an DRI offering both high fringe contrast and high fringe finesse can be made if one will develop a technology for the fabrication of an asymmetric mirror M1C with a matched scatterer.

All-dielectric DRIs with a noninverted shape of spectral dependences of reflectance can be used for radiation selection in short-cavity (< 1 cm) lasers and for obtaining single-frequency lasing. Note that, in contrast to a reflection interferometer based on a thin metallic film [2, 3], DRIs can operate at input powers up to the limiting ones for nonabsorbing dielectric elements under multiple-beam interference conditions (10–100 mW), because the associated losses cause neither heating nor subsequent degradation of the multilayer interferometer structure. If, by analogy with a fibre FPI, one will ensure a means of varying the resonator length of an DRI (e.g. using a linear piezoceramic actuator), it will be possible to tune the laser wavelength over the free spectral range of the DRI, which can be increased to 100 nm or above by reducing the base length l_1 .

6. Conclusions

We have demonstrated an experimental method of obtaining a noninverted interference pattern of an DRI with a high degree of selection in reflected light using only dielectric scattering structures. The characteristics of the DRI can be described analytically by classic formulas of a two-mirror multibeam interferometer, which qualitatively explain measured reflection spectra.

The described DRI can be used as an extracavity fibre (diode) laser frequency selector at output powers from 10 to 100 mW. The reflection interferometer is one of the most effective from the viewpoint of the degree of radiation selection.

To improve parameters of experimental DRIs (fringe finesse and contrast, maximum reflectance), one should determine technological requirements (parameters and their tolerances) for the fabrication of a matched diffraction structure in the input mirror (MIC) that would ensure higher asymmetry of its reflectances. To this end, it is reasonable to perform numerical simulation of an asymmetric mirror based on scattering structures in the fibre eigenmode approximation.

Acknowledgements. This work was supported by the Russian Science Foundation (Project No. 14-22-00118). In our experimental work, we used equipment at the Optics and Spectroscopy Shared Research Facilities Centre, Institute of Automation and Electrometry, Siberian Branch, Russian Academy of Sciences.

References

1. Troitskii Yu.V. *Mnogoluchevye interferometry otrazhennogo sveta* (Multiple-Beam Reflected-Light Interferometers) (Novosibirsk: Nauka, 1985).
2. Terentyev V.S., Simonov V.A., Babin S.A. *Opt. Express*, **24** (5), 4512 (2016), doi:10.1364/OE.24.004512.
3. Terentyev V.S., Simonov V.A., Babin S.A. *Laser Phys. Lett.*, **14**, 25103 (2017), http://dx.doi.org/10.1088/1612-202X/aa548e.

4. Nasim H., Jamil Y. *Laser Phys. Lett.*, **10**, 043001 (2013), doi:10.1088/1612-2011/10/4/043001.
5. Terentyev V.S., Dostovalov A.V., Simonov V.A. *Laser Phys.*, **23**, 085108 (2013), doi:10.1088/1054-660X/23/8/085108.
6. Terentyev V.S., Simonov V.A., Babin S.A. *Opt. Express*, **24** (5), 4512 (2016), doi:10.1364/OE.24.004512.
7. Terentyev V.S., Simonov V.A. *Quantum Electron.*, **46** (2), 142 (2016) [*Kvantovaya Elektron.*, **46** (2), 142 (2016)].
8. Kol'chenko A.P., Terent'ev V.S., Troshin B.I. *Opt. Spectrosc.*, **101** (4), 632 (2006) [*Opt. Spektrosk.*, **101** (4), 674 (2006)], doi: 10.1134/S0030400X06100213.
9. Terentyev V.S., Simonov V.A. *Prikl. Fotonika*, **3** (3), 321 (2016).
10. Marcuse D. *Bell System Tech. J.*, **56** (5), 703 (1977).